



## OPEN

## Effects of water stratification and mixing on microbial community structure in a subtropical deep reservoir

## SUBJECT AREAS:

BIOLIMNOLOGY  
MICROBIAL ECOLOGYReceived  
14 April 2014Accepted  
27 June 2014Published  
25 July 2014Correspondence and  
requests for materials  
should be addressed to  
J.Y. (jyang@iue.ac.cn)Zheng Yu<sup>1,2</sup>, Jun Yang<sup>1</sup>, Stefano Amalfitano<sup>3</sup>, Xiaoqing Yu<sup>1</sup> & Lemian Liu<sup>1</sup><sup>1</sup>Aquatic EcoHealth Group, Key Laboratory of Urban Environment and Health, Institute of Urban Environment, Chinese Academy of Sciences, Xiamen 361021, P. R. China, <sup>2</sup>University of the Chinese Academy of Sciences, Beijing 100049, P. R. China, <sup>3</sup>Water Research Institute, National Research Council of Italy (IRSA-CNR), Monterotondo, Roma, 00015, Italy.

Microorganisms play pivotal roles within aquatic ecosystems, affecting their structure, functioning and services. However, little is known about the effects of water stratification and mixing on the aquatic microbial community dynamics in subtropical reservoirs. In this study, we explored vertical and seasonal patterns of microbial diversity in the Dongzhen Reservoir (southeast China). Quantitative PCR, quantitative RT-PCR, and 454 pyrosequencing were used for an in-depth characterization of the bacterial community across time (every three months for one year) and space (five different water depths). Our results indicated that thermal and oxygen stratification shaped the phylogenetic composition of microbial communities in the reservoir. There were significant differences in physical, chemical and microbiological parameters between epilimnion and hypolimnion ( $P < 0.05$ ). The RNA: DNA ratios were significantly lower in epilimnion and metalimnion but rapidly increased in hypolimnion ( $P < 0.05$ ), suggesting that microorganisms were more active at low temperatures, low dissolved oxygen concentrations and high TN/TP ratios. Redundancy analysis and pathway analysis revealed a complex interplay of various environmental and biological factors by explaining the spatiotemporal variations in bacterial communities. Adaptive reservoir management strategies should consider carefully the effects of water stratification and mixing, together with the distribution patterns of aquatic microorganisms.

Subtropical deep reservoirs are typically characterized by warm monomictic waters showing thermal stratification throughout the year, except for a short mixing period in winter<sup>1,2</sup>. During stratification, surface waters (epilimnion) show higher light intensity, temperatures and dissolved oxygen concentrations in comparison to deep waters (hypolimnion). The upper and lower water layers are separated by the lacustrine interface zone - the metalimnion<sup>3</sup>. During a mixing event after a long period of stratification, nutrients, sulfide, and other dissolved constituents are conveyed to the surface waters, potentially triggering eutrophication processes with direct consequences for ecosystem health status (e.g. algal blooms, odors and fish kills)<sup>4</sup>. Moreover, these contrasting conditions influence the entire aquatic ecosystem functioning<sup>5</sup>. Stratification has important implication for phytoplankton succession, fisheries management, and water supply quality. To prevent the occurrence of excessive nutrient loading, artificial destratification systems are sometimes utilized, but without consistent water quality improvements<sup>6</sup>.

The microbially-driven self-purification processes occurring within the oxygen minimum zone are unquestionably more effective in removing the nutrient excess<sup>7</sup>. In addition, bacteria utilize a wide range of organic compounds (e.g. humic substances) as electron donors for anaerobic respiration, and this, in turn, could lead to increased release of nutrients from sediments under hypoxic conditions<sup>8</sup>. Thus, understanding the spatial and temporal heterogeneity and environmental factors that drive the microbial community structuring in reservoirs is essential for developing effective water quality management approaches<sup>9</sup>.

Microorganisms are well known to serve as the principal producers and decomposers, and play a pivotal role in maintaining freshwater ecosystem health<sup>10</sup>. Several physical, chemical, and biological variables are known to influence the microbial community composition<sup>11,12</sup>. Previous studies showed that the vertical dynamics of the phytoplankton was related to the water column-mixing regime<sup>13</sup>. There appeared to be a subtle interaction between inflows, water column stability, the periodic overturns and the occurrence of the dominant species<sup>14</sup>. While for bacterial community, habitat heterogeneity and seasonal changes can also contribute to community patterns<sup>15</sup>.



Stratification and mixing periods provide a unique opportunity to explore bacterial community responses to both spatial and temporal changes in the environment<sup>16</sup>. Thus, thermal stratified reservoirs represent an ideal system in which to investigate physical and chemical drivers of bacterial community structuring. Previous studies reported major differences in physical and chemical conditions across thermal layers of stratified lakes (epilimnia and hypolimnia) and each layer is known to harbor different bacterial communities<sup>17</sup>. Recently, the rapid development of molecular biological technique has provided powerful tools to specifically explore the aquatic microbial diversity<sup>18,19</sup>.

In this study, a high-throughput sequencing using sequencing-by-synthesis technology was applied as a new approach to exhaustively interpret phylogenetic diversity patterns in microbial communities during stratification and mixing periods. We hypothesized that physical and chemical variables would affect the bacterioplankton diversity at varying extent, and such effects would vary with habitat heterogeneity. Accordingly, our objectives were (i) to examine the effect of water mixing and stratification on the aquatic bacterial diversity, abundance, activity in a subtropical deep reservoir; (ii) to investigate whether the different genera of bacterioplankton coexist together or apart from each other in the different seasons and water depths; and (iii) to investigate the relations between the bacterial community structure and environmental driving factors across time and space.

## Methods

**Study site, sample collection and nucleic acid extraction.** Dongzhen Reservoir (25°29' N, 118°59' E) is located in Putian city, southeast China. The reservoir was built in 1960 with a drainage area of 321 km<sup>2</sup> and a total storage capacity of 435 million m<sup>3</sup>. The sampling station is located in the main lacustrine zone close to the dam where the depth is about 36 m throughout the year. Samples were collected every three months, in October 2011 (autumn), January 2012 (winter), May 2012 (spring), and July 2012 (summer) at five different depths (0, 10, 20, 26 and 33 m), respectively. Each water sample (1 liter with three replications at each depth, maintained at the temperature of 4°C) was immediately sent to the laboratory and filtered onto 0.22-μm pore size polycarbonate membranes (47 mm diameter, Millipore, USA) for the DNA and RNA extraction. The filters were frozen at -80°C until DNA/RNA extraction. Total DNA was extracted from the 0.22-μm filters using a FastDNA spin kit (MP Biomedicals, USA) according to the manufacturer's instructions. Total RNA was extracted from the membranes using the E.Z.N.A. total RNA kit II (Omega Bio-Tek, USA) following the manufacturer's instructions. After the extraction procedure, RNA was transcribed into complementary DNA (cDNA) using the Takara OneStep RT-PCR kit Version 2.0 following the manufacturer's instructions. Reverse transcription was performed as a 15 min reaction at 37°C terminated by 5 s incubation at 95°C. Purified DNA and cDNA were stored at -80°C until further use.

**Physical and chemical analysis.** Water temperature, dissolved oxygen (DO), pH, chlorophyll-*a* (Chl-*a*) and electrical conductivity (EC) were measured in situ at 1-m increments using a multiparameter water quality analyzer (Hydrolab DS5, Hach, USA). Total nitrogen (TN) was determined using a Shimadzu TOC-VCPH analyzer (Shimadzu, Japan). Ammonium nitrogen (NH<sub>4</sub>-N), nitrite and nitrate nitrogen (NO<sub>x</sub>-N) and phosphate phosphorus (PO<sub>4</sub>-P) were measured with a Lachat Qc8500 Flow Injection Analyzer (Lachat Instruments, USA). Total phosphorus (TP) was analyzed by spectrophotometry after digestion. The water column was defined as thermally stratified if temperature difference exceeded by 1°C within 1 m depth at the metalimnion<sup>20</sup>.

**Quantitative PCR and RT-PCR.** PCR amplification of 16S rRNA genes was performed to prepare the quantitative PCR standard curve. The 50-μl PCR mixture contained 1 μl of the primer set (25 pmol each), 0.5 μl (1.25 U) of Ex Taq DNA polymerase (Takara Bio, Japan), 5 μl of Ex Taq buffer, 4 μl of deoxyribonucleotide triphosphate (dNTP) mixture (2.5 mM each), 100 ng of DNA template, and 33.5 μl of ddH<sub>2</sub>O. The primer were 341F (5'- CCTACGGGNGGCWGCAG -3') and 515R (5'- ATTCGCGGCTGGCA -3')<sup>21</sup>. PCR was performed in the following thermal cycles: initial denaturation at 94°C for 5 min; 25 cycles at 94°C for 30 s, 51°C for 30 s and 72°C for 60 s; and a final extension at 72°C for 10 min. The purified PCR products (Promega, USA) were ligated into the pMD18-vector (Takara Bio, Japan) and transformed into *Escherichia coli* DH5α competent cells (Takara Bio, Japan). The plasmids containing 16S rRNA genes fragments were sequenced using an automated sequencer (ABI3730, USA). Successfully inserted plasmids DNA then were extracted using the MiniPrep kit (Qiagen, Germany) and the plasmid concentrations were determined by spectrophotometry using a BioPhotometer (Eppendorf, Germany). Standards were prepared with triplicate from linearized plasmid serial dilutions containing between 10<sup>9</sup> and 10<sup>3</sup> 16S rRNA gene copies calculated directly from the

concentration of extracted plasmid (Table S1). A standard curve was generated by plotting the threshold cycle values versus log<sub>10</sub> of the gene copy numbers. The amplification efficiency (*E*) was estimated using the slope of the standard curve using the following formula:  $E = (10^{-1/\text{slope}}) - 1$ <sup>22</sup>. The efficiency of PCR should be between 95% and 105% for further analysis. The quantitative PCR and RT-PCR assays were carried out in a volume of 20 μl include 10 μl SYBR Premix Ex Taq™, 0.5 μM of each primer, 2 μl of total DNA or cDNA, and RNase-free water. The thermocycling steps of the real-time PCR were run according to the manufacturer's instructions (Takara Bio, Japan). All the measurements were performed in triplicate. In this study, the standard curves with  $r^2 = 0.993 \pm 0.002$  for DNA and  $0.992 \pm 0.002$  for RNA were used as the reference to calculate the concentrations of environmental 16S rDNA and 16S rRNA, respectively. The efficiency of the PCR amplification was  $103.3 \pm 2.3\%$  (16S rDNA) and  $104.2 \pm 0.41\%$  (16S rRNA), respectively. We also compared the ratio of 16S rRNA to 16S rDNA, which is a useful approach to estimate the gene activity of the bacterial community.

**454 pyrosequencing and sequence analysis.** The total DNA was PCR amplified using primers (357F- CCTACGGGAGGCAGCAG and 926R- CCGTCAATTCMTTTRAGT) targeting regions flanking the variable regions 3 through 5 of the bacterial 16S rRNA gene (V3-V5)<sup>23,24</sup>. Each primer set used for PCR amplification contained an eight base DNA bar code for the multiplexing of samples in the pyrosequencing runs<sup>25</sup>. The 50-μl PCR mixture contained 1 μl of the primer set (10 μM each), 0.125 μl (5 U/μl) of Ex Taq DNA polymerase (Takara Bio, Japan), 2.5 μl of Ex Taq buffer (20 mM MgCl<sub>2</sub>), 2 μl of deoxyribonucleotide triphosphate mixture (2.5 mM each, Takara Bio, Japan) and 50 ng of DNA template under the following running conditions: initial denaturation at 94°C for 4 min, 25 cycles of 30 s at 94°C, 45s at 50°C, 1 min at 72°C, and a final elongation step for 8 min at 72°C. PCR products were confirmed using agarose gel electrophoresis and these were subsequently isolated from the gel and purified using a GeneJET™ gel extraction kit (Thermo Fisher Scientific, Germany). All amplicons were pooled in equimolar concentrations, and sent for pyrosequencing on a Roche-FLX+ pyrosequencer at Personal Biotechnology (Shanghai, China). Pyrosequencing reads with more than one 'N' (undetermined nucleotide) and/or those shorter than 200 nt or longer than 1000 nt were removed. Afterwards, primers and barcodes were checked for completeness. Further, the OTUs which contained only 1 read were not used to avoid possible biases, and read with complete barcode sequence was selected for subsequent analysis. Sequences were quality controlled using the Split\_Libraries.py with default settings<sup>5</sup>. Further, any non-bacterial ribosome sequences and chimeras were removed using Black Box Chimera Check software (B2C2) according to the established procedures<sup>26</sup>. Sequences were analyzed using QIIME (v1.0) (based on 97% sequence similarity). The OTUs which contained 1 read were not used to avoid possible sequencing error. Taxonomic classification of the reads was performed in the Ribosomal Database Project (RDP) database<sup>27</sup>. A similarity threshold of 50% in the RDP was applied to assign the reads to the phylum level. The reads of known phyla were further classified into orders<sup>5</sup>.

All sequence data were deposited in the public NCBI database (<http://www.ncbi.nlm.nih.gov/>) under the accession number PRJNA233420.

**Data statistical analysis.** The Shannon-Wiener index (*H'*) was calculated for the 16S rRNA gene diversity. The *H'* was determined with the following equation:  $H' = -\sum P_i \ln P_i$ . The term  $P_i$  was calculated as follow:  $P_i = n_i/N$ , where  $n_i$  is the sequence number of individual OTU and  $N$  is the sequence number of all OTUs in a community<sup>28</sup>. The microbial community compositions in different samples were compared using UniFrac based on the RDP database taxonomic classification<sup>29</sup>. Cluster analysis was used to investigate the phylogenetic composition differences of microbial communities among sites with the program of PRIMER5.0. A group-average linked method was used for Bray-Curtis coefficients among microbial communities in cluster analysis. The normality of the environmental variables and microbial abundance was checked using Shapiro-Wilk test and variables were log( $x + 1$ ) transformed to improve normality and homoscedasticity for multivariate statistical analyses. Analysis of variance (ANOVA) was used in combination with Scheffé's *F* multiple-comparison test to examine differences among the parameters of the sampling sites. Variation partitioning analysis was carried out to assess the individual and combined effects of contextual parameters on changes in bacterial community structure. The gradient length of the longest axis explored by detrended correspondence analysis (DCA) was shorter than 3 SD (standard deviation) units. This indicates that species exhibited linear responses to environmental gradients and thus further analyses were conducted using redundancy analysis (RDA) ordination response models. Environmental variables with variance inflation factors (VIF) < 20 were selected for the following forward selection, and the significance of the conditional effects was detected with 999 Monte Carlo permutations<sup>30</sup>. The variation partitioning analysis was performed on the basis of RDA and pRDA using the R software package with the vegan library. Directed dependencies between the response variables (bacterial community) and all groups of significant relevant contextual parameters were assessed in one causal model with path analysis<sup>31</sup>. The RV coefficient was used to derive a correlation matrix between groups of variables. The Chi-square test was used to assess the adequacy between the overall causal model and the original correlation matrix, in which the *p*-value should not be significant, if the proposed model shows in good agreement with the data. The individual path coefficients indicate the strength of the relation between causal and response variables. The fit of the overall path model was evaluated using the statistical platform R with the *vegan* and *sem* packages<sup>32</sup>.



## Results

**Spatial and temporal environmental heterogeneity.** Dongzhen Reservoir is a typical subtropical warm-monomictic reservoir. The water column was well mixed in winter, whereas the stratification events appeared in spring and lasted until autumn (Figure 1). Interestingly, during stratification, the metalimnion was observed from 2 to 10 m in spring and then dropped to 16 m to 21 m in summer, and then appeared between 24 and 26 m depths in autumn. There were obvious changes in the environmental parameters measured between epilimnion and hypolimnion (Table 1), but little variation was observed during the water mixed period in winter. During stratification, temperature, DO, pH and Chl-*a* were significantly higher in the epilimnion and rapidly dropping down in the hypolimnion ( $P < 0.05$ ). The nutrient concentrations were stable in the water column, except for total phosphorus. Specifically, the TN/TP mass ratio was significantly lower in epilimnion ( $P < 0.01$ ) with mean value of  $79.46 \pm 16.66$  and increased to  $165.62 \pm 29.89$  in hypolimnion. Moreover, the water parameters in summer surface layer (0 m) were different from the other sampling sites; temperature reached the highest value of  $31^\circ\text{C}$ , DO oversaturated with highest concentration of  $11.56\text{ mg/L}$ , pH showed a strong alkalinity at a value of  $10.12$  and the TN/TP mass ratio was as low as  $24.91$ . Furthermore, a significant narrow metalimnion was found from 23 m to 24 m in autumn.

Within the metalimnion range, temperature decreased from  $23^\circ\text{C}$  to  $20^\circ\text{C}$ , and DO changed from  $3.96\text{ mg/L}$  to  $0.24\text{ mg/L}$  (Figure 1).

**Bacterial diversity, abundance and activity.** Bacterial diversity, abundance and activity differed significantly with depth. The Shannon-Wiener diversity index showed a clear increasing trend from epilimnion ( $3.77 \pm 0.13$ ) to hypolimnion ( $4.18 \pm 0.09$ ) with significant difference ( $P < 0.05$ ) (Table 1). For the bacterial abundance, the highest copy number of 16S rDNA was found in the metalimnion with an average value of  $(1.06 \pm 0.14) \times 10^{11}/\text{L}$ . The highest copy number of 16S rRNA reached  $(8.36 \pm 1.36) \times 10^{11}/\text{L}$  in hypolimnion, and there was no difference in 16S rRNA number between epilimnion and metalimnion. Interestingly, the 16S rRNA gene copy numbers in DNA level were generally lower than in RNA level (Figure 2). Further, the RNA: DNA ratios were significantly lower in epilimnion and metalimnion ( $10.59 \pm 2.85$  and  $3.01 \pm 0.64$ , respectively) and rapidly increased in hypolimnion ( $23.17 \pm 3.28$ ), suggesting that bacterial communities were more active in the low temperature, low dissolved oxygen and high TN/TP ratio water zones (hypolimnion).

**Bacterial community composition.** In total, 6068 OTUs with 97% similarity belonging to nine phyla (Actinobacteria, Proteobacteria, Cyanobacteria, Bacteroidetes, Firmicutes, Planctomycetes, Acidobacteria, candidate division WS3 and Verrucomicrobia) were

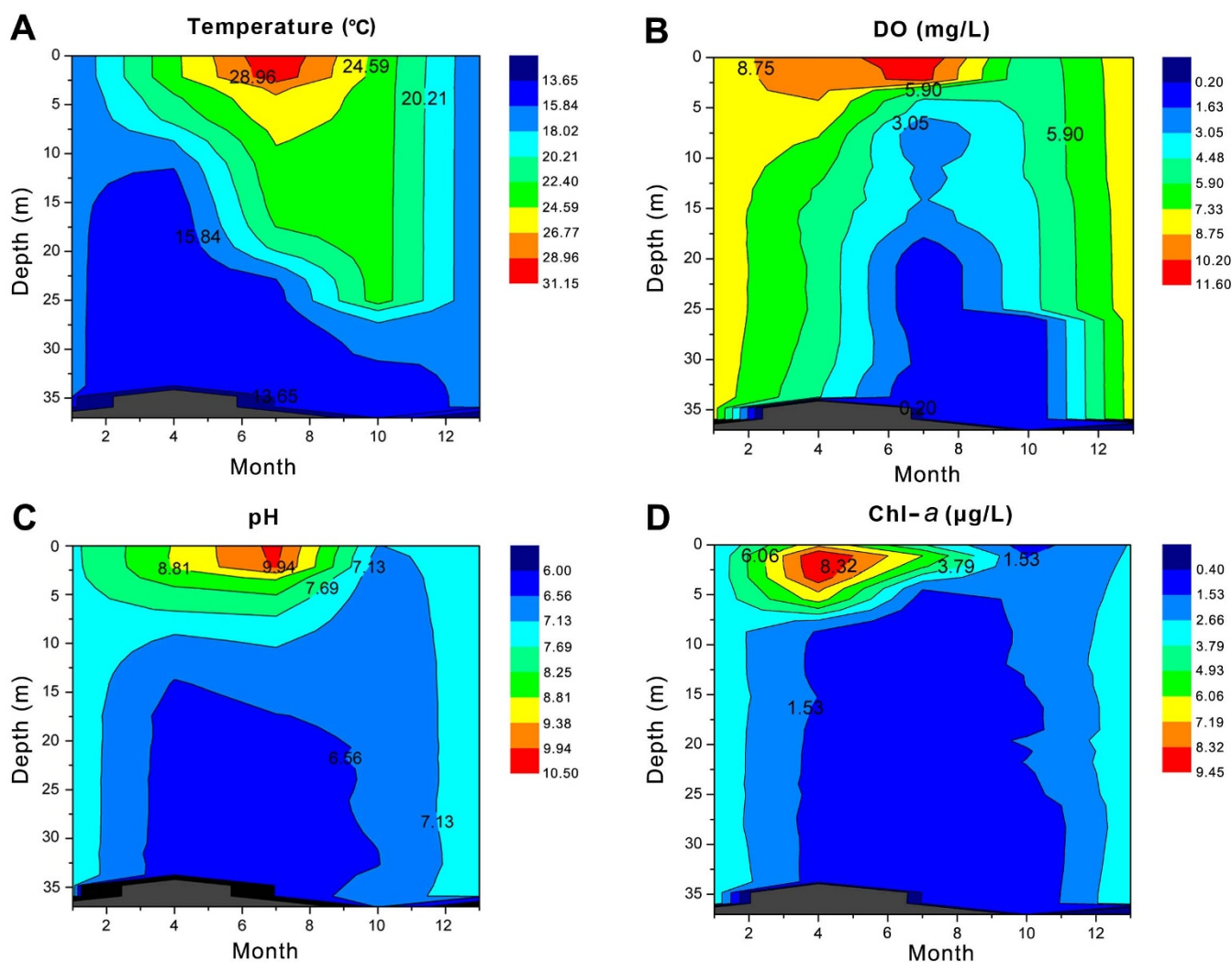


**Figure 1** | (A–D) Temperature, dissolved oxygen (DO), pH and chlorophyll-*a* profiles of Dongzhen Reservoir during one year. The bottom of the reservoir is shown in grey.



**Table 1 | Environmental parameters, Shannon-Wiener index, dominant species' relative abundance and copy number of DNA and RNA in the Dongzhen Reservoir**

Water layer	Mixing layer (n = 5)	Epilimnion (n = 6)	Metalimnion (n = 3)	Hypolimnion (n = 6)
Temperature (°C)	16.17 ± 0.01 <sup>a</sup>	25.04 ± 1.22 <sup>b</sup>	16.87 ± 0.37 <sup>a</sup>	14.18 ± 0.22 <sup>c</sup>
DO (mg l <sup>-1</sup> )	8.23 ± 0.07 <sup>a</sup>	6.16 ± 1.41 <sup>a</sup>	2.26 ± 2.04 <sup>b</sup>	2.82 ± 1.07 <sup>b</sup>
pH	7.46 ± 0.02 <sup>a</sup>	7.75 ± 0.58 <sup>a</sup>	6.64 ± 0.14 <sup>ab</sup>	6.34 ± 0.10 <sup>b</sup>
Chl- <i>a</i> (μg l <sup>-1</sup> )	3.24 ± 0.15 <sup>a</sup>	2.39 ± 0.78 <sup>a</sup>	0.73 ± 0.27 <sup>b</sup>	0.82 ± 0.14 <sup>b</sup>
TN (mg l <sup>-1</sup> )	3.68 ± 0.17 <sup>a</sup>	2.86 ± 0.53 <sup>a</sup>	3.14 ± 1.10 <sup>a</sup>	4.38 ± 1.17 <sup>a</sup>
NH <sub>4</sub> -N (mg l <sup>-1</sup> )	0.10 ± 0.02 <sup>a</sup>	0.18 ± 0.04 <sup>a</sup>	0.13 ± 0.11 <sup>a</sup>	0.20 ± 0.08 <sup>a</sup>
NO <sub>x</sub> -N (mg l <sup>-1</sup> )	1.42 ± 0.06 <sup>a</sup>	1.15 ± 0.14 <sup>a</sup>	1.28 ± 0.18 <sup>a</sup>	1.34 ± 0.10 <sup>a</sup>
TP (mg l <sup>-1</sup> )	0.042 ± 0.008 <sup>a</sup>	0.038 ± 0.004 <sup>ab</sup>	0.026 ± 0.007 <sup>ab</sup>	0.025 ± 0.004 <sup>b</sup>
PO <sub>4</sub> -P (mg l <sup>-1</sup> )	0.002 ± 0.001 <sup>a</sup>	0.009 ± 0.004 <sup>a</sup>	0.014 ± 0.011 <sup>a</sup>	0.011 ± 0.005 <sup>a</sup>
TN/TP mass ratio	100.70 ± 116.94 <sup>ab</sup>	79.46 ± 16.66 <sup>a</sup>	120.99 ± 37.32 <sup>ab</sup>	165.62 ± 29.89 <sup>b</sup>
Shannon-Wiener index	4.00 ± 0.06 <sup>ab</sup>	3.77 ± 0.13 <sup>a</sup>	4.16 ± 0.04 <sup>b</sup>	4.18 ± 0.09 <sup>b</sup>
Actinobacteria (%)	0.706 ± 0.012 <sup>a</sup>	0.625 ± 0.017 <sup>b</sup>	0.629 ± 0.015 <sup>b</sup>	0.589 ± 0.020 <sup>b</sup>
Proteobacteria (%)	0.139 ± 0.006 <sup>a</sup>	0.183 ± 0.023 <sup>a</sup>	0.204 ± 0.036 <sup>a</sup>	0.216 ± 0.014 <sup>a</sup>
Cyanobacteria (%)	0.075 ± 0.004 <sup>a</sup>	0.045 ± 0.025 <sup>ab</sup>	0.033 ± 0.020 <sup>ab</sup>	0.052 ± 0.020 <sup>b</sup>
Unknown bacteria (%)	0.038 ± 0.001 <sup>a</sup>	0.039 ± 0.008 <sup>a</sup>	0.052 ± 0.006 <sup>ab</sup>	0.059 ± 0.006 <sup>b</sup>
Copy number of DNA (l <sup>-1</sup> )	(1.14 ± 0.14) × 10 <sup>10a</sup>	(7.92 ± 1.60) × 10 <sup>10b</sup>	(1.06 ± 0.14) × 10 <sup>11c</sup>	(4.45 ± 0.51) × 10 <sup>10b</sup>
Copy number of RNA (l <sup>-1</sup> )	(6.58 ± 0.16) × 10 <sup>11a</sup>	(3.89 ± 0.72) × 10 <sup>11b</sup>	(2.80 ± 0.60) × 10 <sup>11b</sup>	(8.36 ± 1.36) × 10 <sup>11c</sup>
RNA/DNA ratio	6.31 ± 1.70 <sup>a</sup>	10.59 ± 2.85 <sup>a</sup>	3.01 ± 0.64 <sup>a</sup>	23.17 ± 3.28 <sup>b</sup>

Analysis of variance (ANOVA) was used in combination with Scheffe's F multiple-comparison test to examine differences among the parameters of the sampling sites. Different lower case letters indicate significant differences among the sites. Data represent mean ± SE.

identified. The bacterial community composition differed with depth at the phylum level (Figure 3A). Actinobacteria and Proteobacteria represented the dominant bacterial groups (Figure S1). Actinobacteria showed significantly higher percentages in winter mixing layers ( $0.706 \pm 0.012$ ,  $P < 0.05$ ) than stratification layers (Table 1). Interestingly, the percentage of Cyanobacteria varied rapidly, with values ranging from 16.6% in the spring surface layer (0 m) to 0.24% in the summer deep layer (33 m). In addition, Bacteroidetes bloomed at the summer surface layer (20.8%) but decreased in the low dissolved oxygen environment (Figure 3A). The cluster analysis based on Bray-Curtis coefficient discriminated four groups at the linkage distance of 79.02% (Figure 3B). The summer surface sample formed a distinct cluster. In fact, the defined groups were closely related according to the sampling seasons and depths. It is worth noting that the bacterial composition of Rhizobiales, Burkholderiales, Rhodospirillales, Methylophilales and Legionellales

showed obvious variation associated with water mixing and stratification (Figure S1).

**Relations between microbial community and environmental variables.** Among all environmental variables, only statistically significant environmental variables ( $P < 0.05$ ), including temperature, DO, pH, Chl-*a*, TN and NO<sub>x</sub>-N, were selected in the RDA ordination biplot. The first two RDA dimensions by the six parameters explained 81.7% variation of microbial communities (Figure 4A). Temperature, TN + NO<sub>x</sub>-N and DO + Chl-*a* + pH separately explained 17.5% ( $P = 0.001$ ), 7.4% ( $P = 0.008$ ) and 50.1% ( $P = 0.001$ ) of the variation, respectively. Microbial communities in summer and autumn (positive values of the RDA x-axis) were relatively different from the winter and spring communities (negative values of the RDA x-axis) (Figure 4A).

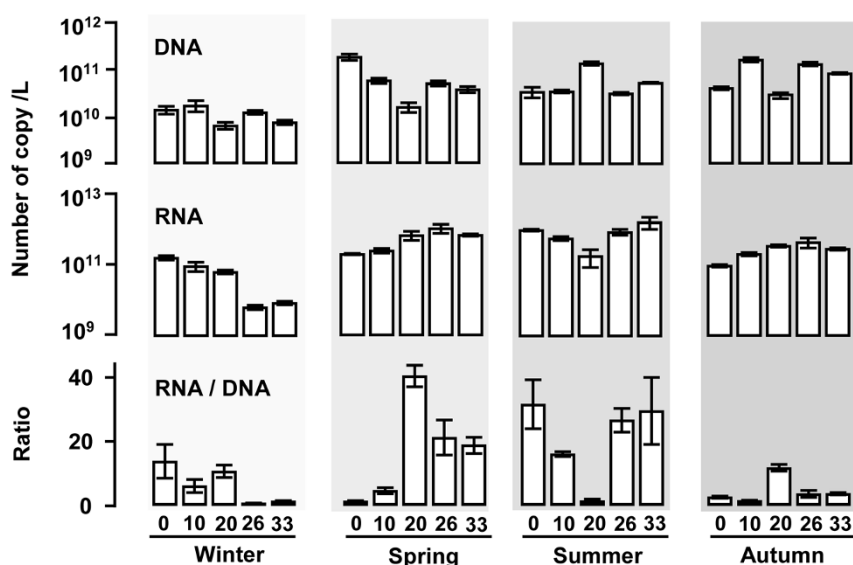


**Figure 2 | Number of 16S rDNA and 16S rRNA copies per liter and RNA: DNA ratio from different water depths (0 m, 10 m, 20 m, 26 m, 33 m) and different seasons (winter, spring, summer, autumn) in Dongzhen Reservoir. Error bars indicate standard errors of the three replicates samples.**

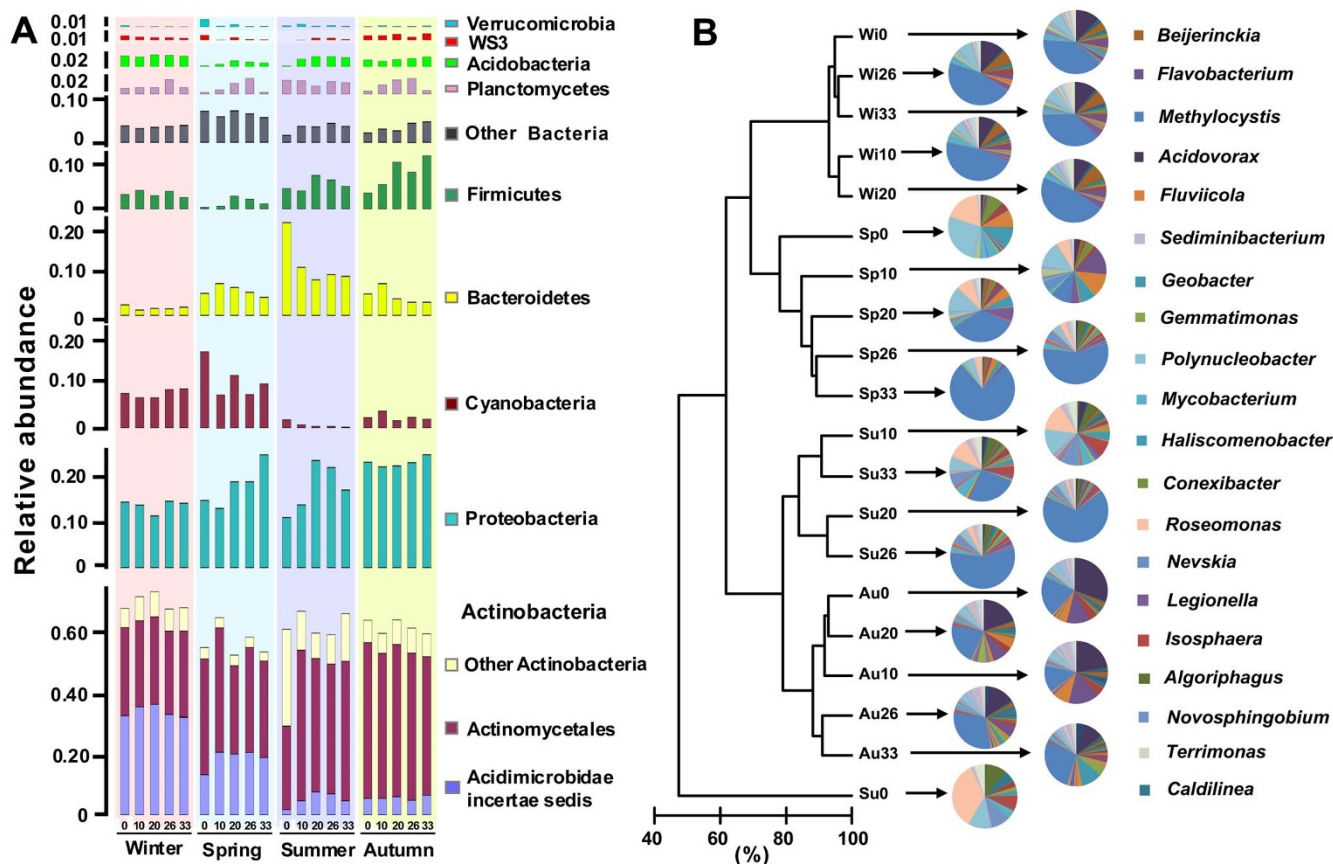


**Figure 3** | (A) Phylum-level (and Actinobacteria class level) changes in different bacterial composition of Dongzhen Reservoir. Relative abundances of phylotyped reads are shown to their closest match in the Ribosomal Database Project. (B) Cluster analysis of bacterial communities based on the Bray-Curtis similarity of 454 pyrosequencing profiles. The right legend shows color-coding indicating the top 20 most abundant genera in Dongzhen Reservoir.

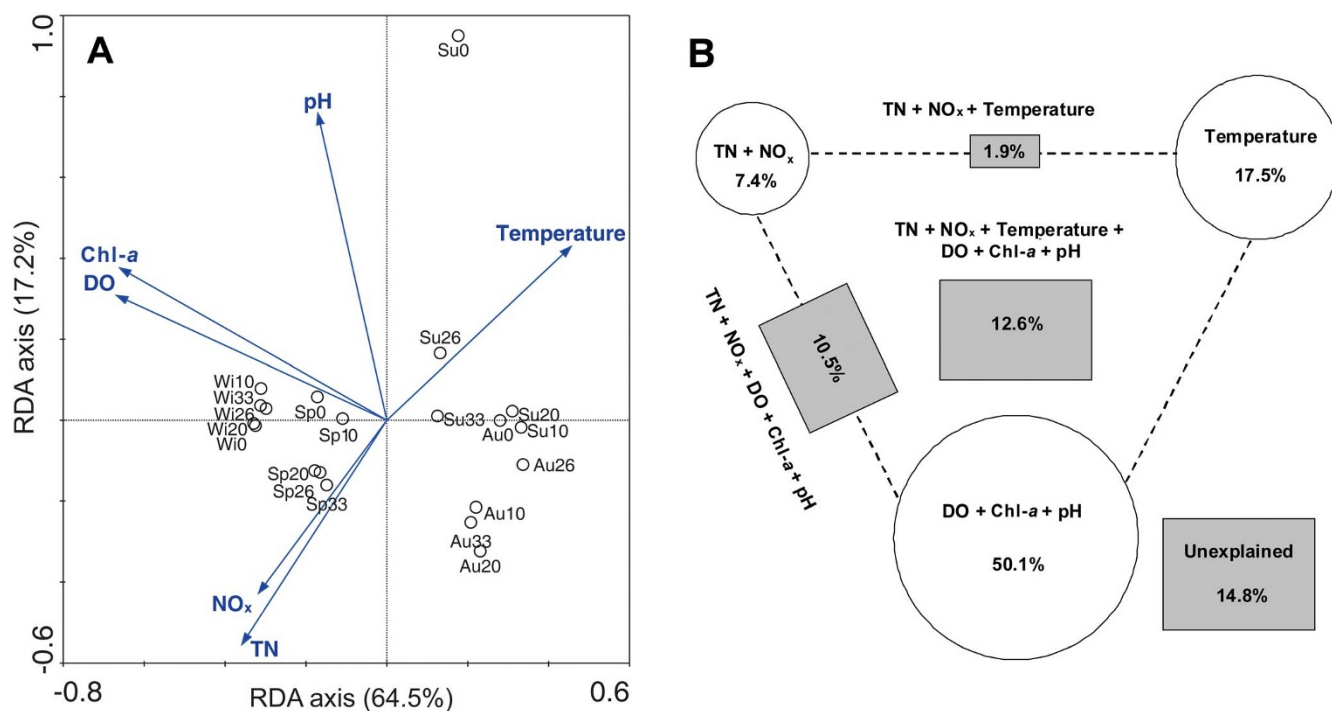


**Figure 4** | (A) RDA biplot of the distribution of bacterial community and environmental variables in Dongzhen Reservoir. Only statistically significant environmental variables are shown according to Monte Carlo permutation test ( $P < 0.05$ ). (B) Variation partitioning of bacterial communities into the statistically significant environmental variables.



Pathway analysis was applied to examine microbial communities and reciprocal interactions in their microhabitats. The significance value for the Chi-square test was 0.293, indicating that the proposed model was in good agreement with the data. The goodness-of-fit index and Bentler CFI (Comparative fit index) = 1 indicated a better fit and thus our model was the best fitting model. The Bayesian Information Criterion (BIC) was 28.07, and the minimized value obtaining the better model fit was given (Figure 5). Thus, our results showed that there were demonstrably stark distinctions in physical and chemical conditions across thermal layers in the reservoir.

## Discussion

Deep reservoirs represent attractive ecosystems in which to explore the influence of habitat heterogeneity on microbial community assembly because of their unique mixing and stratification dynamics<sup>16</sup>. In this study, we analyzed whether spatial and temporal variations in physical and chemical conditions may be associated with changes in bacterial diversity and community composition. Our results showed that bacterial communities were structurally different between the different water layers of a subtropical deep reservoir. The abiotic and biotic niche diversification, related to water stratification events, could explain the microbial community dynamics across time and space<sup>33</sup>.

In the Dongzhen Reservoir, we found significant differences in physical (water temperature and DO), chemical (pH, TN, TP and TN/TP ratio) and microbiological (Chl-*a*, community composition and gene copy number) parameters between epilimnion and hypolimnion (Table 1). Qian *et al.* (2011) proved that the variation in the microbial communities with depth could be attributable to their adaptations to the various environments<sup>5</sup>. The thermocline depth is known to be an important factor for microbial community structuring in aquatic ecosystems, particularly for bacterioplankton and phytoplankton groups with limited motility<sup>34,35</sup>. In agreement with previous reports, cluster analysis results clearly showed that the bacterial community composition in the same season was strongly associated with water stratification (Figure 3B). Water stratified isolation, physiological characteristics, and ecological traits could work together to limit bacterioplankton dispersal<sup>36</sup>. There have been various theoretical predictions for the differential success of micro-organism groups to constraints imposed by habitat heterogeneity in freshwater ecosystems, based on competitive abilities for energy

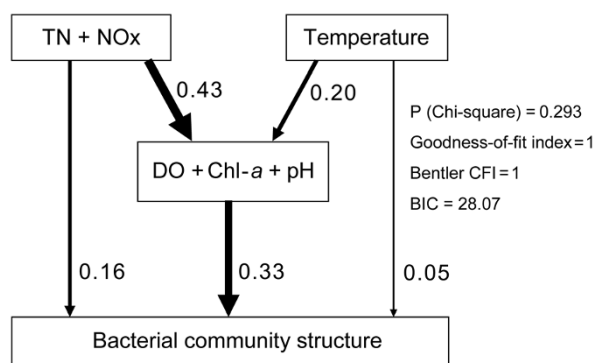


**Figure 5 | Final path with structural equation modeling.** The significant value for the Chi-square test is given, assessing whether the model is significantly different from the corresponding correlation matrix. The goodness-of-fit index and Bentler CFI (Comparative Fit Index) indicate the goodness of fit of the model, the best fit would result in a value of 1. The Bayesian Information Criterion (BIC) is another measure of the goodness-of-fit and it is minimized to obtain a better model fit. Numbers on each arrow indicate partial correlation coefficients associated with each causal relationship, and arrow thickness is also proportional to the partial correlation value.

availability and nutrient acquisition<sup>16,37</sup>. It was suggested that high local diversity could be maintained under intermediate levels of physical disturbance<sup>38</sup>. Moreover, low and high levels of disturbance are expected to be less effective in maintaining a high diversity because the former enables competitive exclusion and the latter directly eliminates many species<sup>39</sup>.

In this study, Actinobacteria, Proteobacteria and Cyanobacteria were the most dominant groups within the analyzed waters. Despite being mainly found in soils<sup>40</sup>, members of Actinobacteria are recognized as ubiquitous and abundant in lake waters according to recent molecular-based studies<sup>10</sup>. They can contribute to more than 50% of the total bacteria in surface waters (epilimnion), but often decrease with decreasing oxygen concentrations in the bottom waters (hypolimnion) of lakes and reservoirs<sup>41</sup>. Within aquatic bacterial communities, Proteobacteria represent the largest and phenotypically most diverse phylogenetic lineage<sup>42</sup>. Herein, five subdivisions of Proteobacteria were recognized. Alphaproteobacteria, mainly belonging to two genera (*Methylocystis* and *Roseomonas*), and Betaproteobacteria, mainly belonging to two genera (*Acidovorax* and *Polynucleobacter*), were the most abundant groups. Cyanobacteria acting as primary producers were dominant in spring surface waters, but declined sharply in summer and autumn deep water. The ability of Cyanobacteria to perform photosynthesis and nitrogen fixation in the presence of light and oxygen can explain the dominance of this group in the surface waters<sup>43</sup>.

Our results showed that structural patterns of bacterial communities were related to temperature and nutrient profiles in the stratified water column (Figures 4 and 5). The warmer surface waters re-circulated in the epilimnion, without mixing with the colder and dense waters of the hypolimnion<sup>2</sup>. Thus, deep waters remained isolated from dissolved oxygen inputs, leading to hypoxic conditions in the hypolimnion. When a mixing event occurred after a long period of stratification, nutrients and other dissolved constituents were conveyed to the upper portion of the water column, leading to water quality deterioration<sup>4,44</sup>. Since bacteria drive the organic matter breakdown and nutrient remineralization<sup>45</sup>, the dominant bacterial metabolic pathways were likely to regulate the solute circulation within different water layers. Temperature differences affected the water density and then led to physical and chemical stratification, which could further contribute to niche differentiation in the water column. Niche differentiation apparently shaped bacterial community and this in turn affected the water quality<sup>46,47</sup>.

Previous researches demonstrated that the water quality may be adversely affected if prolonged stratification occurs in lakes and reservoirs<sup>48,49</sup>. In this scenario, a holistic, ecosystemic, and integrated understanding of the responses of aquatic microbial communities to varying environmental conditions should be considered for establishing appropriate management approaches for water resources protection<sup>9</sup>.

1. Wang, S., Qian, X., Han, B. P., Wang, Q. H. & Ding, Z. F. Physical limnology of a typical subtropical reservoir in south China. *Lake Reserv. Manage.* **27**, 149–161 (2011).
2. Elçi, Ş. Effects of thermal stratification and mixing on reservoir water quality. *Limnology* **9**, 135–142 (2008).
3. Becker, V., Huszar, V. L. M. & Crossetti, L. O. Responses of phytoplankton functional groups to the mixing regime in a deep subtropical reservoir. *Hydrobiologia* **628**, 137–151 (2009).
4. Lawson, R. & Anderson, M. A. Stratification and mixing in Lake Elsinore, California: an assessment of axial flow pumps for improving water quality in a shallow eutrophic lake. *Water Res.* **41**, 4457–4467 (2007).
5. Qian, P. Y. *et al.* Vertical stratification of microbial communities in the Red Sea revealed by 16S rDNA pyrosequencing. *ISME J.* **5**, 507–518 (2011).
6. Vandermeulen, H. Design and testing of a propeller aerator for reservoirs. *Water Res.* **26**, 857–861 (1992).
7. Pantoja, S., Sepúlveda, J. & González, H. E. Decomposition of sinking proteinaceous material during fall in the oxygen minimum zone off northern Chile. *Deep Sea Res. Pt. I* **51**, 55–70 (2004).



8. Coates, J. D., Cole, K. A., Chakraborty, R., O'Connor, S. M. & Achenbach, L. A. Diversity and ubiquity of bacteria capable of utilizing humic substances as electron donors for anaerobic respiration. *Appl. Environ. Microbiol.* **68**, 2445–2452 (2002).
9. Yang, J., Yu, X. Q., Liu, L. M., Zhang, W. J. & Guo, P. Y. Algae community and trophic state of subtropical reservoirs in southeast Fujian, China. *Environ. Sci. Pollut. Res.* **19**, 1432–1442 (2012).
10. Newton, R. J., Jones, S. E., Eiler, A., McMahon, K. D. & Bertilsson, S. A guide to the natural history of freshwater lake bacteria. *Microbiol. Mol. Biol. R.* **75**, 14–49 (2011).
11. Liu, L. M., Yang, J., Yu, X. Q., Chen, G. J. & Yu, Z. Patterns in the composition of microbial communities from a subtropical river: Effects of environmental, spatial and temporal factors. *PLoS ONE* **8**, e81232 (2013).
12. Lv, H., Yang, J. & Liu, L. M. Temporal pattern overwhelms spatial variability in phytoplankton communities from a subtropical water supply reservoir. *Oceanol. Hydrobiol. St.* **42**, 420–430 (2013).
13. Xiao, L. J. *et al.* Succession of phytoplankton functional groups regulated by monsoonal hydrology in a large canyon-shaped reservoir. *Water Res.* **45**, 5099–5109 (2011).
14. Borges, P. A. F., Train, S. & Rodrigues, L. C. Spatial and temporal variation of phytoplankton in two subtropical Brazilian reservoirs. *Hydrobiologia* **607**, 63–74 (2008).
15. Laque, T., Farjalla, V., Rosado, A. & Esteves, F. Spatiotemporal variation of bacterial community composition and possible controlling factors in tropical shallow lagoons. *Microb. Ecol.* **59**, 819–829 (2010).
16. Shade, A., Jones, S. E. & McMahon, K. D. The influence of habitat heterogeneity on freshwater bacterial community composition and dynamics. *Environ. Microbiol.* **10**, 1057–1067 (2008).
17. Boucher, D., Jardillier, L. & Debroas, D. Succession of bacterial community composition over two consecutive years in two aquatic systems: a natural lake and a lake-reservoir. *FEMS Microbiol. Ecol.* **55**, 79–97 (2006).
18. Hamady, M. & Knight, R. Microbial community profiling for human microbiome projects: tools, techniques, and challenges. *Genome Res.* **19**, 1141–1152 (2009).
19. Lauber, C. L., Zhou, N., Gordon, J. I., Knight, R. & Fierer, N. Effect of storage conditions on the assessment of bacterial community structure in soil and human-associated samples. *FEMS Microbiol. Lett.* **307**, 80–86 (2010).
20. Wilhelm, S. & Adrian, R. Impact of summer warming on the thermal characteristics of a polymictic lake and consequences for oxygen, nutrients and phytoplankton. *Freshwater Biol.* **53**, 226–237 (2008).
21. Lane, D. J. 16S/23S rRNA sequencing. In: Stackebrandt E, Goodfellow M (eds). *Nucleic Acid Techniques in Bacterial Systematics*. John Wiley and Sons: Chichester. pp 115–175 (1991).
22. Bustin, S. A. *et al.* The MIQE guidelines: minimum information for publication of quantitative real-time PCR experiments. *Clin. Chem.* **55**, 611–622 (2009).
23. Humblot, C. & Guyot, J. P. Pyrosequencing of tagged 16S rRNA Gene amplicons for rapid deciphering of the microbiomes of fermented foods such as Pearl Millet slurries. *Appl. Environ. Microbiol.* **75**, 4354–4361 (2009).
24. Vilo, C. & Dong, Q. Evaluation of the RDP classifier accuracy using 16S rRNA gene variable regions. *Metagenomics* **1**, 1–5 (2012).
25. Hoffmann, C. *et al.* DNA bar coding and pyrosequencing to identify rare HIV drug resistance mutations. *Nucleic Acids Res.* **35**, e91 (2007).
26. Gontcharova, V. *et al.* Black box chimera check (B2C2): a windows-based software for batch depletion of chimeras from bacterial 16S rRNA gene datasets. *Open Microbiol. J.* **4**, 47–52 (2010).
27. Crawford, P. A. *et al.* Regulation of myocardial ketone body metabolism by the gut microbiota during nutrient deprivation. *Proc. Nat. Acad. Sci. USA* **106**, 11276–11281 (2009).
28. Haegeman, B. *et al.* Robust estimation of microbial diversity in theory and in practice. *ISME J.* **7**, 1092–1101 (2013).
29. Lozupone, C. & Knight, R. UniFrac: a new phylogenetic method for comparing microbial communities. *Appl. Environ. Microbiol.* **71**, 8228–8235 (2005).
30. Xu, M. Y. *et al.* Responses of microbial community functional structures to pilot-scale uranium in situ bioremediation. *ISME J.* **4**, 1060–1070 (2010).
31. Bienhold, C., Boetius, A. & Ramette, A. The energy-diversity relationship of complex bacterial communities in Arctic deep-sea sediments. *ISME J.* **6**, 724–732 (2012).
32. Sawall, Y., Richter, C. & Ramette, A. Effects of eutrophication, seasonality and macrofouling on the diversity of bacterial biofilms in equatorial coral reefs. *PLoS ONE* **7**, e39951 (2012).
33. Becker, V., Huszar, V. L. M., Naselli-Flores, L. & Padisák, J. Phytoplankton equilibrium phases during thermal stratification in a deep subtropical reservoir. *Freshwater Biol.* **53**, 952–963 (2008).
34. Berdjeb, L., Ghiglione, J. F. & Jacquet, S. Bottom-up versus top-down control of hypo- and epilimnion free-living bacterial community structures in two neighboring freshwater lakes. *Appl. Environ. Microbiol.* **77**, 3591–3599 (2011).
35. Cantin, A., Beisner, B. E., Gunn, J. M., Prairie, Y. T. & Winter, J. G. Effects of thermocline deepening on lake plankton communities. *Can. J. Fish. Aquat. Sci.* **68**, 260–276 (2011).
36. Ghiglione, J. F. *et al.* Pole-to-pole biogeography of surface and deep marine bacterial communities. *Proc. Nat. Acad. Sci. USA* **109**, 17633–17638 (2012).
37. Fazi, S., Vázquez, E., Casamayor, E. O., Amalfitano, S. & Butturini, A. Stream hydrological fragmentation drives bacterioplankton community composition. *PLoS ONE* **8**, e64109 (2013).
38. Connell, J. Diversity in tropical rain forests and coral reefs. *Science* **199**, 1302–1310 (1978).
39. Li, Z. *et al.* Responses of phytoplankton diversity to physical disturbance under manual operation in a large reservoir, China. *Hydrobiologia* **684**, 45–56 (2012).
40. Rheims, H., Felske, A., Seufert, S. & Stackebrandt, E. Molecular monitoring of an uncultured group of the class Actinobacteria in two terrestrial environments. *J. Microbiol. Meth.* **36**, 65–75 (1999).
41. Glöckner, F. O. *et al.* Comparative 16S rRNA analysis of lake bacterioplankton reveals globally distributed phylogenetic clusters including an abundant group of actinobacteria. *Appl. Environ. Microbiol.* **66**, 5053–5065 (2000).
42. Pinhassi, J. & Berman, T. Differential growth response of colony-forming  $\alpha$ - and  $\gamma$ -proteobacteria in dilution culture and nutrient addition experiments from Lake Kinneret (Israel), the eastern Mediterranean Sea, and the Gulf of Eilat. *Appl. Environ. Microbiol.* **69**, 199–211 (2003).
43. Yu, Z. *et al.* Water stratification affects the microeukaryotic community in a subtropical deep reservoir. *J. Eukaryot. Microbiol.* **61**, 126–133 (2014).
44. Rigosi, A. & Rueda, F. J. Hydraulic control of short-term successional changes in the phytoplankton assemblage in stratified reservoirs. *Ecol. Eng.* **44**, 216–226 (2012).
45. Weston, N. B. & Joye, S. B. Temperature-driven decoupling of key phases of organic matter degradation in marine sediments. *Proc. Natl. Acad. Sci. USA* **102**, 17036–17040 (2005).
46. Shade, A. *et al.* Resistance, resilience and recovery: aquatic bacterial dynamics after water column disturbance. *Environ. Microbiol.* **13**, 2752–2767 (2011).
47. Shade, A. *et al.* Lake microbial communities are resilient after a whole-ecosystem disturbance. *ISME J.* **6**, 2153–2167 (2012).
48. Boehrer, B. & Schultze, M. Stratification of lakes. *Rev. Geophys.* **46**, RG2005 (2008).
49. Comeau, A. M., Harding, T., Galand, P. E., Vincent, W. F. & Lovejoy, C. Vertical distribution of microbial communities in a perennially stratified Arctic lake with saline, anoxic bottom waters. *Sci. Rep.* **2**, 604 (2012).

## Acknowledgments

This work was supported by the National Basic Research Program of China (2012CB956103), the National High-Tech Research and Development Program of China (2012AA062607), the National Natural Science Foundation of China (31172114 and 31370471) and the Natural Science Foundation for Distinguished Young Scholars of Fujian Province (2012J06009). We thank David M. Wilkinson for polishing the English of the manuscript.

## Author contributions

Conceived and designed the experiments: J.Y. and Z.Y. Performed the experiments: Z.Y. Analyzed the data: Z.Y. and J.Y. Contributed reagents/materials/analysis tools: Z.Y., J.Y., S.A., X.Y. and L.L. Wrote the paper: Z.Y. and J.Y. All authors reviewed the manuscript.

## Additional information

**Supplementary information** accompanies this paper at <http://www.nature.com/scientificreports>

**Competing financial interests:** The authors declare no competing financial interests. All of the authors agree to the submission of this paper. Neither the entire paper nor any part of its content has been published elsewhere.

**How to cite this article:** Yu, Z., Yang, J., Amalfitano, S., Yu, X. & Liu, L. Effects of water stratification and mixing on microbial community structure in a subtropical deep reservoir. *Sci. Rep.* **4**, 5821; DOI:10.1038/srep05821 (2014).



This work is licensed under a Creative Commons Attribution-NonCommercial-NoDerivs 4.0 International License. The images or other third party material in this article are included in the article's Creative Commons license, unless indicated otherwise in the credit line; if the material is not included under the Creative Commons license, users will need to obtain permission from the license holder in order to reproduce the material. To view a copy of this license, visit <http://creativecommons.org/licenses/by-nc-nd/4.0/>